processes

MDPI

Article

Supercritical Fluid Extraction of Peruvian *Schinus molle* Leaves: Yield, Kinetics, Mathematical Modeling, and Chemical Composition

Joselin Paucarchuco-Soto [1], German Padilla Pacahuala [1], Walter Javier Cuadrado Campó [1], Perfecto Chagua-Rodríguez [1], Julio Cesar Maceda Santivañez [1,2], Ádina L. Santana [3], Maria Angela A. Meireles [1,4] and Larry Oscar Chañi-Paucar [1,*]

[1] Grupo de Investigación en Ingeniería de Alimentos y Agroindustria (GIIAA), Universidad Nacional Autónoma Altoandina de Tarma (UNAAT), La Florida-Cochayoc Highway, 2092 Huancucro, Junin 12651, Peru
[2] Mass Spectrometry and Chemical Ecology Laboratory (MS-CELL), Center for Natural and Human Sciences, Federal University of ABC, UFABC, Av dos Estados 5001–Bangú, Santo André 09280-560, SP, Brazil
[3] Grain Science and Industry Department, Kansas State University, 1301 N Mid Campus Drive, Manhattan, KS 66506, USA
[4] School of Food Engineering, University of Campinas (UNICAMP), R. Monteiro Lobato 80, Campinas 13083-862, SP, Brazil
* Correspondence: larry.76728@gmail.com or lchani@unaat.edu.pe

Abstract

According to the literature, *Schinus molle* (SM) is an important source of bioactive phytochemicals, but the phytochemical content and composition of this species, which grows in high Andean geographic zones such as Tarma (Peru), is not known. In an effort to fill this gap, our work investigated the supercritical carbon dioxide extraction of SM leaves at three temperature levels (35, 45, and 55 °C) and three pressure levels (150, 250, and 350 bar). The results revealed the highest yield of extract at 150 bar, 45 °C, and 3.28 g CO_2/min. Under these conditions, the overall extraction curves (OEC) were modeled using the Spline, logistic, and Esquível models, allowing the generation of mass transfer parameters for SFE at the optimized conditions, resulting in a similar correlation with experimental data. Twenty-six compounds were identified in the SFE extract of SM leaves. The most abundant compound classes were sesquiterpenoids (57.17%), sesquiterpenes (24.50%), and triterpenoids (10.48%); of each class, the most abundant compounds were shyobunol (33.60%), bicyclogermacrene (12.68%), and lupeone (6.58%), respectively. The compounds detected possess bioactive properties that support further studies on the application of SFE extracts of SM as a functional ingredient in commercial products.

Keywords: Andean aromatic plants; supercritical fluid extraction; mathematical modeling; volatile compounds; aromatic compounds

check for updates

Academic Editor: Agnieszka Zgoła-Grześkowiak

Received: 13 May 2025
Revised: 30 June 2025
Accepted: 3 July 2025
Published: 9 July 2025

Citation: Paucarchuco-Soto, J.; Padilla Pacahuala, G.; Cuadrado Campó, W.J.; Chagua-Rodríguez, P.; Maceda Santivañez, J.C.; Santana, Á.L.; Meireles, M.A.A.; Chañi-Paucar, L.O. Supercritical Fluid Extraction of Peruvian *Schinus molle* Leaves: Yield, Kinetics, Mathematical Modeling, and Chemical Composition. *Processes* **2025**, *13*, 2191. https://doi.org/10.3390/pr13072191

Copyright: © 2025 by the authors. Licensee MDPI, Basel, Switzerland. This article is an open access article distributed under the terms and conditions of the Creative Commons Attribution (CC BY) license (https://creativecommons.org/licenses/by/4.0/).

1. Introduction

Schinus molle L. (SM) is an aromatic arboreal species found in the Peruvian Andes and other regions of South America [1]. Although there is a large number of scientific reports on the bioactive potential of the phytochemicals produced by this species, there are still limited studies of plants growing in the high Andean zones of Peru.

It has been reported that SM contains essential oils, which are traditionally extracted by hydrodistillation from its aerial parts [2,3], leaves [4], fruits [4,5], and resins [6]. SM

essential oil has potential applications, such as insecticide [7], antioxidant [8,9], bactericide [10,11], herbicide [2,6], anti-corrosive [12], and fungicide [13]. The bioactive properties of SM essential oil have demonstrated potential in the production of biocidal microcapsules [14] and intelligent/active food packaging films [15]. According to scientific reports, the chemical composition of essential oils in SM parts differs in terms of the concentration of major compounds present. For instance, in SM leaves the compounds detected include α-phellandrene (29.8%), β-phellandrene (21.1%) and elemol (13.0%) [16]; α-phellandrene (20.3%), d-limonene (16.4%), germacrene-D (15.5%), and bicyclogermacrene (12.3%) [6]; 1R-α-pinene (15.5%), camphene (14.0%), β-myrcene (11.5%), and o-cymene (29.0%) [11]; 1-tetradecene (43.3%) and 1-dodecanol (22.8%) [7]; limonene (22.9%), α- and β-terpinene (12.0%) [4]; there are other compositions reported by other authors [8–10,13,17,18]. However, the major compounds in SM essential oil extracted from resin included caryophyllene (18.3%), bicyclogermacrene (9.2%), and germacrene-B (20.2%) [6]. In the essential oil extracted from SM fruits, the major compounds found were limonene (22.9%) [4], β-myrcene (35.8%), α-phellandrene (20.6%), and D-limonene (19.4%) [15]. The differences in the chemical composition of SM essential oils reported are attributed to the geographical area and growing conditions of the crops produced [5] and the method of extraction [8].

SM is also an interesting source of non-volatile bioactive compounds, such as alkaloids, and flavonoids [19,20]. These compounds can be present in the aerial part [21], fruits [22], husks [22], unpeeled fruits [22], stem bark [23], flowers [24], leaves [19], and seeds [20,25], which have been extracted with solvents like water [26,27], aqueous ethanol [21,28], hexane [25,29], dichloromethane [25,30], ethyl acetate [30], methanol [19], aqueous methanol [20], petroleum ether [24], acetone [24], diethyl ether [24], and solvent mixtures [31]. Solvent extraction of SM parts has been performed using traditional methods, such as maceration [23,24], boiling [26], infusion [32], and immersion warming [21]. The extracts obtained with the reported methods presented the following properties: wound-healing [21], antimicrobial [21,23], antiviral [27], antioxidant [28], antidiabetic [32], anti-inflammatory [28,33], antinociceptive [33], anticancer [24,29], antimalarial [20], antidiarrheal [19,34], analgesic [35], cytotoxic [31], gastroprotective [25], and hepatoprotective [19]. Besides the bioactive properties of SM extracts, the chemical composition of SM allowed its processing into nanoparticles with antioxidant [30] and anticancer [26] potentials. The diverse properties already reported are attributed to the wide range of molecules found in SM, including alkaloids [35], flavonoids [35], tannins [29], triterpenes [25], sequiterpenes [29], and other chemical components [20].

Currently, several emerging and eco-friendly technologies have been implemented for the extraction of bioactive compounds to overcome the time and solvent-consuming attributes of traditional methods [36]. The potential of supercritical fluid extraction (SFE) as an eco-friendly method for selecting bioactive compounds to replace petroleum-derived solvents and producing extracts without contamination has been demonstrated [37,38]. The SFE of bioactive compounds from SM has been studied in mixtures of leaves and branches [39,40] and leaves [41], utilizing carbon dioxide (CO_2) as the primary supercritical fluid.

Barroso et al. [39] reported that for the SFE of SM (2 mm average particle diameter) at the conditions of 9–20 MPa, 50 °C, and CO_2 flow rate of 8.3 g/min, the higher yield was obtained at 15 MPa, and the quality of extracts consisted of high proportions of limonene (41.4%), (E)-caryophyllene (15.6%), and bicyclogermacrene (11.6%). Marongiu et al. [40] reported α-phellandrene (26.5%), limonene + β-phellandrene (22.2%), elemol (10.8%), and α-eudesmol (6.0%) as major compounds of SM leaves extracts obtained at 9 MPa, 50 °C, and 16.7 g/min. According to our literature review, the extraction of bioactive compounds using supercritical fluid extraction (SFE) with CO_2 is promising. However, additional studies are

required to investigate a wider range of thermodynamic parameters, as these can influence yield and composition, as observed in other raw materials [42,43]. Mathematical modeling of the overall extraction curves (OEC) generated from supercritical fluid extraction (SFE) is useful for process design and optimization, as it enables the assessment of kinetic behavior, aiding in the decision-making process for selecting the optimal processing parameters to achieve optimized extract quality and processing time. The OEC of the SFE process of clove and sugarcane residues at the laboratory and pilot scales were adequately described [41]. Studies on the characterization and potential applications of SM grown in the geographical area of Tarma, Peru, are scarce, to the best of the authors' knowledge. For this reason, the goal of this work was to evaluate the recovery of extracts from SM leaves collected in Tarma Province, Peru, using supercritical fluid extraction (SFE) via a 3^2-factorial design and mathematical modeling of overall extraction curves (OEC) using empirical models. The chemical composition of extracts obtained under best yield conditions was evaluated using gas chromatography-mass spectrometry (GC–MS) to assess the bioactive potential of the extracts.

2. Materials and Methods

2.1. Raw Material

Samples of SM were collected for botanical identification (collection coordinates: 11°27′32″ S and 75°40′49″ W) and extraction experiments (collection coordinates: 11°26′20″ S and 75°41′30″ W) in the district of Tarma, Junin, Peru. Dr. Carlos Reynel Rodríguez identified the species, and a botanical sample was deposited in the herbarium located at the Faculty of Forestry Sciences in the Universidad Nacional Agraria la Molina (Peru), with the sample code 52114. The use of this species for scientific investigation was authorized by the Servicio Nacional Forestal y de Fauna Silvestre—SERFOR (RA Nº D000260-2024-MIDAGRI-SERFOR-ATFFS-SELVA CENTRAL).

2.1.1. Preparation

SM leaves were dried and covered in Kraft paper at room temperature until they achieved a dried and brittle texture. Dried SM leaves (DSML) were vacuum-packed and stored at −20 °C (Meling Biomedical, DW-YL270, Hefei, China). The leaves were then ground using a home immersion blender (Oster FPSTHB460A-053, 400 W, China) for 60 s.

2.1.2. Particle Size

The particle size of SM was determined by inserting 30 g of dried and milled raw material into a granulometry analyzer (Retsch, AS 200 Basic, Haan, Germany) [42].

2.1.3. Colorimetric Analysis

The colorimetric analysis of DLSM was determined in the solid material before and after the SFE, with a portable colorimeter (Konica Minolta, CR-20, Japan) under the CIE L*a*b* system. With the lightness (L*) and the coordinates (a* for red (+) or green (−), and b* for yellow (+) or blue (−)), the color variations were calculated, i.e., ΔL*, Δa*, Δb* and ΔE*. The parameter ΔE* consists of the total color difference, as described in Equation (1).

$$\Delta E^* = \left[(\Delta L^*)^2 + (\Delta a^*)^2 + (\Delta b^*)^2 \right]^{0.5} \quad (1)$$

2.2. SFE Equipment

A bench-scale SFE equipment (Singularity Extraction Technologies, PD-Basic-2235, Campinas, Brazil) was used (Figure 1). The equipment was located at the Instituto de Investigaciones en Tecnologías Altoandinas (INITA) of the Universidad Nacional Autónoma

Altoandina de Tarma (UNAAT), at an altitude of 3053 m above mean sea level (AMSL). Under the ambient conditions attributed (17 °C was considered) to the geographical zone from where the experiments were performed, the CO_2 density considered was 1.257 kg/m^3, according to the NIST website [43]. The SFE unit compressor was operated with the aid of a cooling bath (Singularity Extraction Technologies, Brazil) at −2 °C and a medical-grade air compressor (SCHULZ, MSV 12, SCHULZ Compressores LTDA, Santa Catarina, Brazil) supplying air at 4 bar. The CO_2 flow was controlled with the aid of a flowmeter (MasterFlex, IL, USA). The volume of CO_2 used in each extraction was measured in cubic meters with the aid of a totalizer (LAO, G1,6, São Paulo, Brazil).



Figure 1. SFE unit at the laboratory scale (Singularity Extraction Technologies, Campinas, Brazil).

2.3. SFE Experiments

2.3.1. Experimental

Carbon dioxide (99.99% purity, Linde, Lima, Peru) was the solvent used in SFE. The experiments were carried out in an extraction vessel (100 mL, 31.38 mm diameter) loaded with 10.03 ± 0.01 g of DLSM and glass beads (3 mm diameter, ISOLAB Laborgeräte GmbH, Carsalo, Brazil) to fill the empty spaces. SFE experiments were conducted to determine the conditions of highest extraction yield, based on a 3^2-factorial design, evaluating the effects of pressure (150, 250, and 350 bar) and temperature (35, 45, and 55 °C) on extraction yield. Nine experiments were performed in duplicate. A CO_2 flow rate of 3.28 g/min, a static time of 10 min, and a solvent to feed ratio (S/F, g CO_2/g feedstock) of 11.87 were selected. Global yield (or yield of extract) was determined gravimetrically, according to Equation (2), where Y is the yield of extract from DLSM obtained via SFE (expressed in %, g/100 g), E is the weight of extract obtained from the SFE (expressed in g), and S is the weight of raw material (DLSM) used in the extractions (expressed in g).

$$Y\left(\frac{g}{100g}\right) = \frac{E}{S} \times 100 \quad (2)$$

2.3.2. Overall Extraction Curves and Mathematical Modelling

The overall extraction curve (OEC) was plotted for the process conditions associated with the highest extract yield, as determined by the assays in Section 2.3.1. Duplicate OECs were performed using 10.03 ± 0.01 g of DLSM, and extracts were collected periodically for up to 140 min of extraction. For the collection of extracts, 50 mL vials were used.

The OEC of SM extraction was plotted considering the extraction yield (g extract per 100 g raw material) versus the solvent-to-feed ratio (S/F, g CO_2/g raw material). The kinetic behavior was studied by modeling the OEC using empirical models [38,44–47].

The Visual Basic for Applications function of Microsoft Excel was used to model the 2 straight-lines spline [38,45,46]. The solver function of Microsoft Excel estimated the adjustable parameters for logistic model, implemented by Martínez et al. [44], and Esquível et al. model [47]. The Spline model [38,46] is expressed by the Equation (3):

$$m_{EXT} = b_0 + b_1 t + b_2 (t - t_{CER}) \quad (3)$$

where

b_0 (g) is the linear coefficient, b_1 (or M_{CER}, in g/min) is the slope of constant extraction rate (CER) straight period, physically expressed as M_{CER}, which is the extraction rate for the CER period; b_2 (or M_{FER}, in g/min) is the slope of falling extraction rate (FER) straight line; m_{EXT} (g) is the mass of extract, t is the time of extraction (min), and t_{CER} (min) is CER period.

The mass of extract predicted at the CER period (R_{CER}, g extract/100 g raw material) was calculated by dividing the ratio between the accumulated mass of extract at t_{CER} and the mass of feed F_0 (g), as demonstrated in Equation (4).

$$R_{CER} = \left(\frac{m_{CER}}{F_0} \right) \times 100 \quad (4)$$

The mass ratio of extract in the supercritical phase at the vessel outlet (Y_{CER}, g extract/g CO_2) was calculated as the ratio between b_1 (or M_{CER}) and the CO_2 flow.

Martinez et al. [44] proposed a logistic model (Equation (5)) to describe the OECs, considering the mass transfer of the extract (represented by a single group of compounds) to the fluid phase.

$$m_{EXT} = \frac{X_0 F_0}{\exp(bt_m)} \left\{ \frac{1 + \exp(bt_m)}{1 + [\exp(t_m - 1)]} - 1 \right\} \quad (5)$$

where m_{EXT} is the mass of extract (g), F_0 (g) is the input mass of raw material, X_0 is the global yield expressed in terms of m_{EXT}/F_0 (g/g), b (m^{-1}), and t_m (min) are the adjustable parameters.

Esquível et al. [47] proposed an empirical equation (Equation (6)) to predict the yield variation in the SFE.

$$m_{EXT} = X_0 F_0 \left(\frac{t}{b + t} \right) \quad (6)$$

where m_{EXT} is the mass of extract (g), F_0 is the mass of raw material used in the SFE (g), t (min) is the time of extraction (min), and b (min) is the adjustable parameter of the model with no physical meaning.

2.4. Characterization of Extract

Gas Chromatography–Mass Spectrometry (GC–MS)

The chemical composition of the DLSM SFE extract was assessed by gas chromatography-mass spectrometry (GC–MS). The analysis service was performed by the Laboratory of Research and Certifications (LABICER) of the National University of Engineering (UNI). A gas chromatograph GC–2010 Plus (Shimadzu, Kyoto, Japan), equipped with autosampler

AOC-6000 (Shimadzu, Japan), mass spectrometer GCMS-QP210 Ultra (Shimadzu, Japan), and RESTEK Rtx-5 MS column (30 m × 0.25 mm × 0.25 µm) was used. The analysis was performed following the chromatographic method developed by Bendif et al. [48], considering an interface temperature of 290 °C and 250 °C for the ion source. Before analysis, 0.1 mL of the DLSM SFE extract was diluted in 9.9 mL of n-hexane (Merck Millipore, EMSURE, Darmstadt, Germany) and filtered (0.45 µm syringe filter: Nylon Filter, TEKNOKROMA, Barcelona, Spain). Helium (≥99.99% purity, Linde Peru S.R.L., Peru) was used as carrier gas. The compounds were identified using the NIST 2014 library, which is available in the software provided with the equipment. The relative composition (expressed as percentage, %) was determined by dividing the chromatographic peak area of the single compound by the areas of all chromatographic peaks detected, followed by multiplication of the resulting value by 100.

2.5. Statistical Analysis

The effect of pressure and temperature on the extraction yield was evaluated using a 3^2-factorial design. The results were evaluated to determine the assumptions of normality (using the Anderson–Darling test) and homogeneity of variance (using the Bartlett test). Subsequently, analysis of variance (ANOVA) was performed at a significance level of 0.05 using Minitab software version 21.2 (Minitab LLC, USA).

3. Results and Discussions

3.1. Effect of SFE Parameters

Extractions were performed with ground DLSM with an average particle diameter of 0.82 ± 0.01 mm. An average particle diameter (2 mm) was used in the extraction of bioactive from SM samples (leaves and twigs) with supercritical CO_2 [39]. The reduction in the particle size contributes to the extraction of bioactive, because the grinding allows to break the structures of the plant material. The effects of experimental conditions on the yield of extract are shown in Figure 2. The highest yield of 1.36 ± 0.03% was observed at 150 bar and 45 °C, and the lowest yield of 0.88 ± 0.08% was observed at 150 bar and 55 °C. Interestingly, the yields obtained in this work were higher than those reported by Marongiu et al. [40], who observed yield of 0.7% after the SFE of SM leaves at 90 bar, 50 °C and 16.67 g CO_2/min, and slightly lower compared to those reported by Barroso et al. [39], who conducted SFE of a mixture of SM leaves and twigs at the conditions of 120 bar, 50 °C and 8.28 g CO_2/min per 120 min, and by Scopel et al. [49], after the SFE with pure CO_2 at 150 bar, 60 °C and 8.28 g CO_2/min for 170 min. According to Scopel et al. [49], the use of a cosolvent (water and ethanol) in SFE with CO_2 did not increase the yield of *Schinus molle* extract (leave + twigs). On the other hand, extraction with the use of cosolvents affects bioactive properties, such as antimicrobial activity [49]. The yield of bioactive extract obtained from DLSM observed in the present study and its difference with that reported in the literature show that the SM species growing in the high Andean region of central Peru is a potential source of bioactive. The differences observed are probably due mainly to the genetic variability of the species and the area of cultivation.

Considering the effect of temperature, it was observed that for the isotherms obtained at 35 and 55 °C, the extraction yield was higher at 250 bar. However, it was also observed that 45 °C significantly decreased the extract yield at 250 bar, which is attributed to the increased vapor pressure of target molecules present in the SM extract, leading to a decrease in the CO_2 solvation power [50]. However, after increasing the pressure to 350 bar, a considerable increase in the extraction yield was observed at 45 °C, as the system had overcome the crossover region under these conditions. The crossover region consists of the overlap of solubility of the extract in CO_2 as the temperature increases [51]. At

150 bar, it was observed that the extract yield increased after the temperature increased from 35 to 45 °C, and then decreased with further temperature increases from 45 to 55 °C. This phenomenon occurred because at pressures lower than the crossover pressure (in this work, possibly between 250 and 350 bar), the effect of CO_2 density predominates in the extraction. For instance, at 150 bar, the density of CO_2 at 45 °C is approximately 0.742 g/mL, which is next to the densities of alcohols used in conventional extraction of essential oils like methanol (0.792 g/mL), which explain the affinity of extract to CO_2 at the selected condition compared to 55 °C, where the density of CO_2 is 0.654 g/mL [52].

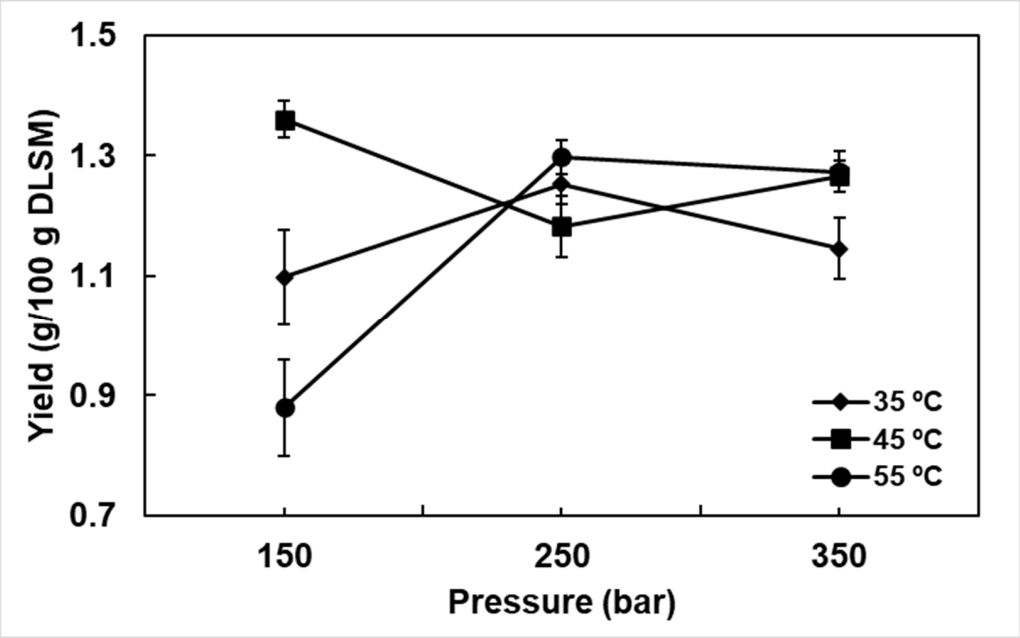


Figure 2. DLSM extract yield at different temperatures and pressures: with a CO_2 flow rate of 3.28 g/min, S (g CO_2)/F (g DLSM) of 11.87, and 36.29 min of extraction.

The normality analysis of experimental errors follows a normal distribution according to Anderson–Darling's normality test at a significance level of 0.05 (p-value = 0.106 and Anderson–Darling's statistic was 0.592). On the other hand, the analysis of the homogeneity of variances using the Bartlett statistic (α = 0.05) showed homogeneity across variances (p-value = 0.972 and Bartlett statistic = 2.25). Therefore, the results of the test of normality and homogeneity of variations suggest that it is pertinent to proceed with the analysis of variations to determine whether there is a significant effect in terms of individual or interaction of factors (pressure and temperature) on the DLSM extract yield. Table 1 presents the ANOVA results for the extract yield obtained under various experimental conditions. The results of the ANOVA, with α = 0.05, indicate that the interaction between temperature and pressure levels has a significant effect (p-value = 0.00) on the yield of the DLSM extract (Table 1). Likewise, temperature and pressure have a significant individual effect on the extract yield. The effect of the thermodynamic variables in the SFE process can vary depending on the raw material, as in the case of the extraction of oil from sucupira seeds, it was reported that the temperature × pressure interaction were not significant effect on the yield [53], a similar observation was carried out in samples of *Acca sellowiana* (O. Berg) Burret [54].

Table 1. Analysis of variance (ANOVA) on the effects of temperature and pressure of SFE.

Source	DF	Seq SS	Contribution (%)	Adj SS	Adj MS	F-Value	*p*-Value
T	2	0.05065	14.43	0.05065	0.025325	10.03	0.005
P	2	0.06213	17.70	0.06213	0.031064	12.30	0.003
T × P	4	0.21553	61.40	0.21553	0.053883	21.34	0.000
Error	9	0.02272	6.47	0.02272	0.002525		
Total	17	0.35103	100.00				

T: temperature, °C; P: pressure, bar; DF: degrees of freedom; Seq SS: sequential sums of squares; Adj SS: adjusted sums of squares; Adj MS: adjusted mean squares.

The dried and milled SM leaves, as well as the extract collected under optimal conditions (45 °C and 150 bar), are shown in Figure 3. The extract (Figure 3) has an amber coloration and an oily texture. The oily texture of the SM extract is due to the fat-soluble nature of its major compounds, such as the sesquiterpenoid [55]. A pale yellow color was observed in a fraction of the SM leaves extract obtained with supercritical CO_2 at 90 bar and 50 °C [40]. The fractionation of the SM extract performed by Marongiu et al. [40], could explain the difference in the color of the extract obtained by these authors and us. On the other hand, the color of leaves before and after SFE under the optimal conditions is observed in Figure 3B and C. The colorimetric analysis of SM leaves after the SFE increased the lightness (L* coordinate, Table 2), decreased the green color coordinate (a*, Table 2), and increased the yellow color (b* coordinate, Table 2). Such color variations are potentially attributed to the extraction of pigments during SFE.

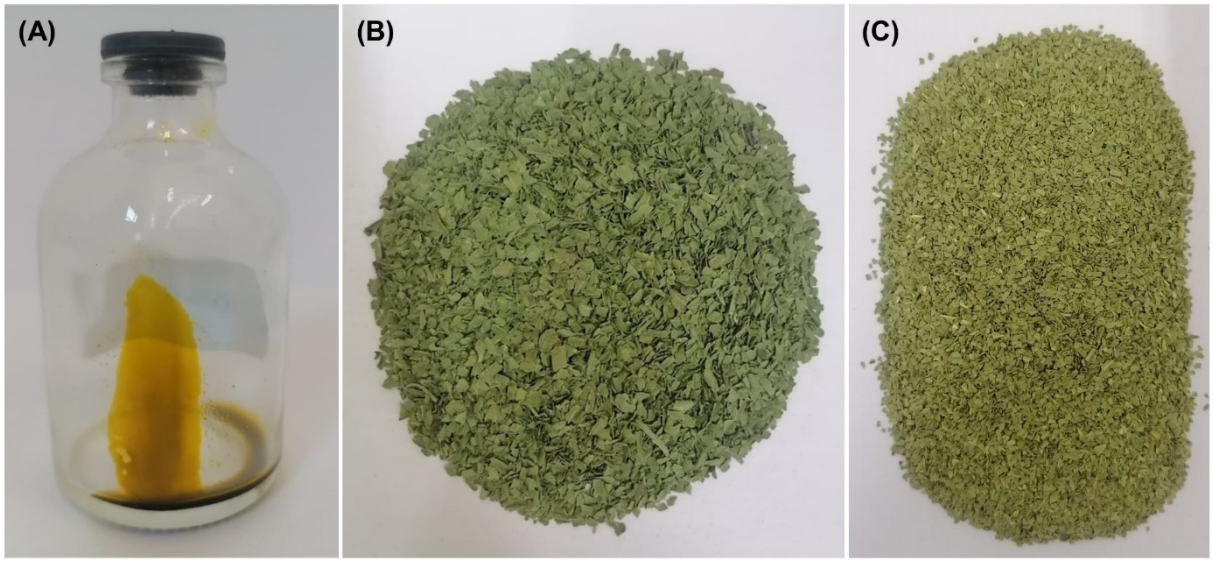


Figure 3. The extract (**A**), dried leaves of *S. molle* before (**B**) and after (**C**) SFE extraction at 45 °C and 150 bar.

Table 2. CIELAB parameters of DLSM, before and after SFE extraction at 45 °C and 150 bar.

DLSM	CIELAB Parameters						
	L*	ΔL*	a*	Δa*	b*	Δb*	ΔE*
Before extraction	39.19 ± 0.24	39.21	−4.26 ± 0.17	0.41	18.85 ± 0.15	15.48	42.16
After extraction [56]	78.40 ± 0.16		−3.85 ± 0.18		34.33 ± 0.23		

3.2. Mathematical Modeling

Figure 4 shows the OCE of DLSM, plotted as cumulative yield versus extraction time and cumulative yield versus S/F. The adjustable parameters for the mass transfer models, along with the correlation factor and mean square errors (MSE) obtained for each model, are presented in Table 3. The lowest deviation between experimental and correlated data was obtained by the Spline model (Table 3). Despite the highest correlation factor (R^2), the Esquível model showed the highest deviation between the experimental and predicted data, compared to the Spline, indicating that R^2 alone does not fully describe the model's ability to predict the OEC. The Esquível model predicts the OEC, like the variation in mass of extract absorbed with adsorbate pressure given by the Langmuir isotherm. Martinez et al. [44] propose a model that uses the logistic growth equation to describe OECs, considering the solute as a pseudo-pure component.

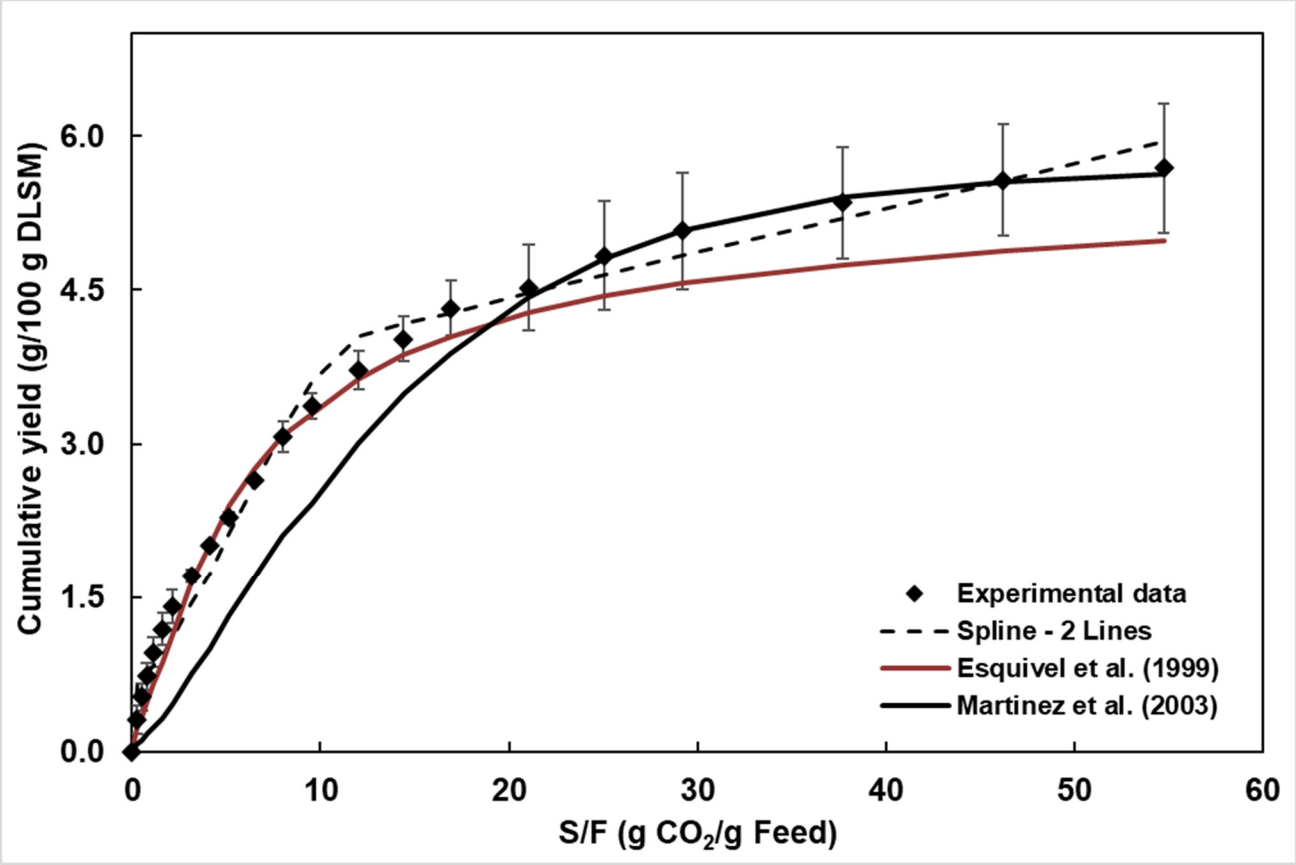


Figure 4. Cumulative yield of DLSM extract obtained at 45 °C and 150 bar (experimental data [56]) and curves of the fitted mathematical models, at 3.28 g CO_2/min and S/F of 54.8 [44,47].

The Esquível et al. [47] and Martínez et al. [44] models present a few adjustable parameters: b (min) for the Esquível model and b (min^{-1}) and t (min) for the Martínez model. For this reason, these models do not provide sufficient information to describe the types of mass transfer mechanisms involved in the supercritical fluid extraction (SFE) of solid matrices. Additionally, the lack of physical meaning of the parameters renders these types of models inapplicable for process design and scale-up, despite serving as a simple alternative to describe the evolution of the SFE process using empirical kinetic equations.

Table 3. The adjustable parameters, mean square error (MSE), and correlation factor (R^2) of mass transfer models applied to the SC-CO_2 extraction of *S. molle* at 45 °C and 15 MPa.

Model	Parameters	Result
Spline	t_{CER} (min)	27.00
	b_0 (g/min)	5.507×10^{-3}
	$b_1 = M_{CER}$ (g/min)	3.875×10^{-3}
	$b_2 = M_{FER}$ (g/min)	-3.343×10^{-3}
	R_{CER} (% g ext/100 g feed)	4.052
	Y_{CER} (g ext/g CO_2)	1.178×10^{-3}
	R^2	0.984
	MSE	3.95×10^{-4}
Esquível	b (min)	99.08
	R^2	0.994
	MSE	7.6×10^{-4}
Martínez	t_m (min)	1.0×10^{-11}
	b (min^{-1})	2.279
	R^2	0.985
	MSE	4.26×10^{-3}

Considering the Spline model, the duration of the CER period (t_{CER}) was 27 min (Table 3). In the CER period, represented by the first adjusted line, occurs the extraction of the soluble material available on the surface of the plant matrix. The R_{CER} of 4.052 g/100 g corresponded to approximately 70% of the experimental global yield of 5.56 g/100 g obtained for the experimental OEC, which is consistent with the literature, which states that during the CER period, approximately 70–90% of the soluble material is extracted [46].

This result is relevant for the further scale-up techno-economic assessment of *Schinus molle* (SM) leaf extraction via SFE. Key factors such as overall extraction yield, extract quality, and processing costs are critical factors in decision making for industrial implementation. Compared to traditional methods such as distillation, these factors become even more significant. It is important to note that, although general economic trends for SFE are documented, its economic feasibility varies on a case-by-case basis, because of raw material properties, process conditions, location, and market factors [57].

The interpretation for the negative b_2 (or M_{FER}, in Table 3) is that neither external nor internal diffusion mass transfer mechanisms are relevant to the OEC.

3.3. SFE Extract Composition

The relative composition of DLSM SFE extract obtained at 45 °C and 150 bar is available in Table 4. In the extract chromatogram, a prominent presence of shyobunol, bicyclogermacrene, elemol, lupeone, germacrene D-4-ol, and gamma-Gurjunene was observed (Figure 5). Shyobunol was the major compound in the extract studied in this work. Interestingly, this compound was found in the lowest amounts in the SFE extracts of SM at 90 bar and 50 °C [39], and in *Citrus limon* (L.) Osbeck essential oil [58] and different parts of Bolivian SM [59]. Bicyclogermacrene is the second major compound in the DLSM SFE extract, whose presence was reported previously in the SM essential oils extracted via SFE from the leaves [39,41], and resin [6]. Bicyclogermacrene is a compound also found in *Heracleum sprengelianum* leaves, which presented larvicide activity [60]. Other important compounds found in the DLSM SFE extract include: (a) elemol, found previously in SM in essential oil [8,13,16,18,40] and SFE extract [40], which has been applied as repellant agent against ticks [61], (b) lupeone, a compound detected in the extracts of *Boscia coriacea* (Pax.)

peels, showed anticancer potential [62], (c) germacrene D-4-ol, found in the essential oil of *Artemisa* species, that showed larvicide activity against *Aedes aegypti* L. [63], (d) gamma-Gurjunene, a compounds found at highest amount in *Pluchea indica* (L.) Less. tea [64]. The DLSM SFE extract obtained presents molecules with important bioactive properties and has the potential to be used as an ingredient in products for the chemical, cosmetic, and pharmaceutical industries.

Table 4. Composition of the SFE extract of *S. molle* leaves obtained at 45 °C and 150 bar.

RT [a]	Compounds [a]	MF	MW	Area (%) [a]	Some Bioactive Properties/Uses [b]
7.073	Alpha Phellandrene (M)	$C_{10}H_{16}$	136.23	0.19	
7.983	Pseudolimonene (M)	$C_{10}H_{16}$	136.23	0.17	
19.226	Gamma-Elemene (S)	$C_{15}H_{24}$	204.35	1.17	Antileishmanial activity [65]
21.050	Beta-Elemene (S)	$C_{15}H_{24}$	204.35	1.15	Antiangiogenic activity [66]
21.591	Alpha-Gurjunene (S)	$C_{15}H_{24}$	204.35	0.51	
21.887	Caryophyllene (S)	$C_{15}H_{24}$	204.35	1.83	Insecticidal activity [67]
22.959	Humulene (S)	$C_{15}H_{24}$	204.35	0.63	
23.194	9-epi-(E)-Caryophillene (S)	$C_{15}H_{24}$	204.35	0.34	
23.828	Germacrene D (S)	$C_{15}H_{24}$	204.35	0.26	
24.323	Bicyclogermacrene (S)	$C_{15}H_{24}$	204.35	12.68	Larvicide [60]
24.457	Alpha-Muurolene (S)	$C_{15}H_{24}$	204.35	0.20	
24.893	Cubebol (St)	$C_{15}H_{26}O$	222.37	0.59	
25.012	Not identified	-	-	4.54	
25.183	6-epi-shyobunol (St)	$C_{15}H_{26}O$	222.37	4.35	
25.914	Elemol (St)	$C_{15}H_{26}O$	222.37	10.42	Repellent [61] Fragrance [68]
26.416	Palustrol (St)	$C_{15}H_{26}O$	222.37	0.30	
26.661	Germacrene D-4-ol (St)	$C_{15}H_{26}O$	222.37	6.31	
27.124	Viridiflorol (St)	$C_{15}H_{26}O$	222.37	0.80	
27.242	Not identified	-	-	0.71	
27.453	Ledol (St)	$C_{15}H_{26}O$	222.37	0.48	
28.193	Epiglobulol (St)	$C_{15}H_{26}O$	222.37	0.32	
29.274	Not identified	-	-	0.74	
29.916	Shyobunol (St)	$C_{15}H_{26}O$	222.37	33.60	
32.231	Gamma-Gurjunene (S)	$C_{15}H_{24}$	204.35	5.73	
33.018	Not identified	-	-	1.02	
47.281	Linolenic acid (Fa)	$C_{18}H_{30}O_2$	278.4	0.09	
50.602	Squalene (T)	$C_{30}H_{50}$	410.7	0.36	
56.688	Beta-Amyrone (Tp)	$C_{30}H_{48}O$	424.7	3.28	
57.110	Beta-Amyrin (Tp)	$C_{30}H_{50}O$	426.7	0.62	
57.564	Lupeone (Tp)	$C_{30}H_{48}O$	424.7	6.58	
	Total area			99.97	

MF: molecular formula, MW: molecular weight, RT: retention time (min), M: monoterpene, S: sesquiterpene, St: sesquiterpenoid, FA: fatty acid, T: triterpene, and Tp: triterpenoid. [a] Paucarchuco Soto and Padilla Pachuala [56]. [b] Reported in the scientific literature.

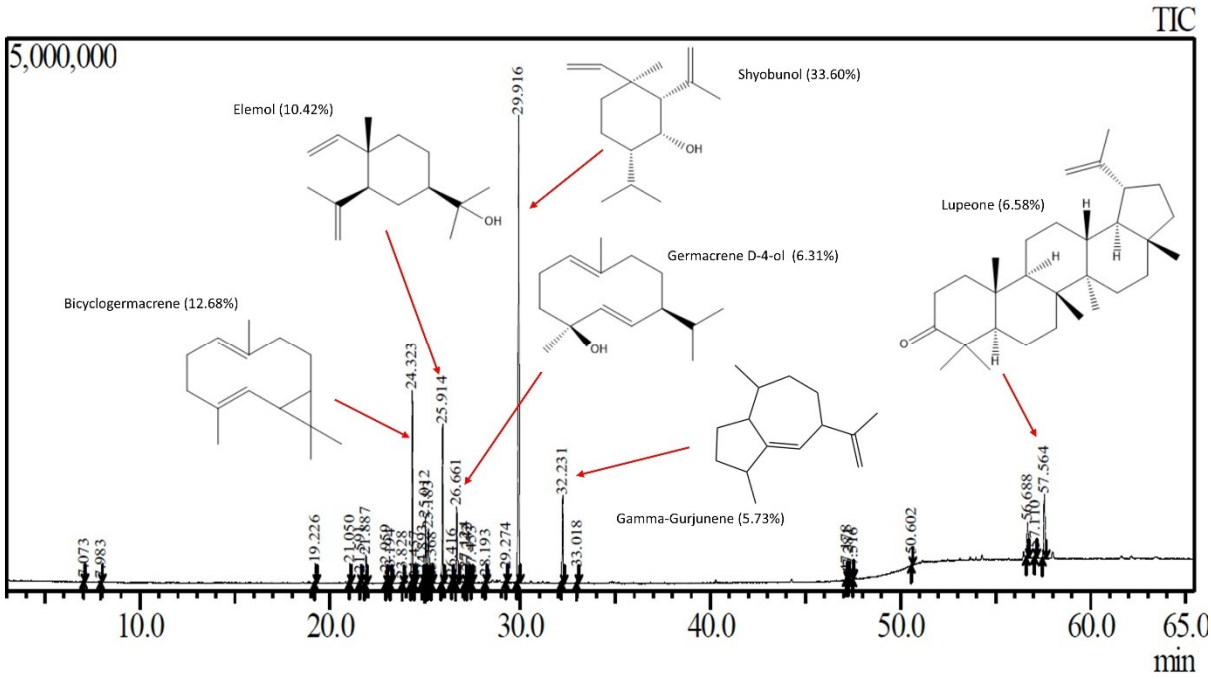


Figure 5. Chromatogram of the SFE extract of *S. molle* and main compounds identified. Adapted from the author's graduate work [56].

4. Conclusions

This work studied the extraction of *S. molle* leaves using supercritical fluid extraction (SFE). The extraction yields were affected by the temperature and pressure of supercritical CO_2; the highest and lowest yields were observed under conditions of 150 bar and 45 °C, and 150 bar and 55 °C, respectively. Under the highest yield conditions, it was possible to obtain 5.69% *w*/*w* extract from the DLSM for an S/F of 54.8 and 140 min of extraction. The Spline model precisely described the OECs plotted under the conditions of best extraction yield with two straight lines. The model calculated the duration of the constant extraction rate to be 27 min, during which approximately 70% of the total extract yield was obtained. The SFE extract consisted mainly of sesquiterpenoids, sesquiterpene, and triterpenoids. The compounds identified in the present study possess diverse bioactive properties, according to the scientific literature, suggesting their potential for the functional products industry. Our results show that the SFE extract of *S. molle* leaves produced in Tarma, Peru, has potential to be used as an ingredient in products with functional properties.

Author Contributions: Conceptualization, J.P.-S., G.P.P. and L.O.C.-P.; Methodology, J.P.-S., G.P.P., W.J.C.C., P.C.-R., J.C.M.S., Á.L.S. and L.O.C.-P.; Validation, L.O.C.-P.; Formal analysis, J.P.-S., G.P.P. and L.O.C.-P.; Investigation, G.P.P., M.A.A.M. and L.O.C.-P.; Data curation, J.P.-S., G.P.P. and L.O.C.-P.; Writing—original draft, J.P.-S., G.P.P., W.J.C.C., P.C.-R., J.C.M.S., Á.L.S. and L.O.C.-P.; Writing—review & editing, J.P.-S., G.P.P., W.J.C.C., P.C.-R., J.C.M.S., Á.L.S. and L.O.C.-P.; Visualization, L.O.C.-P.; Supervision, W.J.C.C., M.A.A.M. and L.O.C.-P.; Project administration, W.J.C.C., M.A.A.M. and L.O.C.-P.; Funding acquisition, M.A.A.M. and L.O.C.-P. All authors have read and agreed to the published version of the manuscript.

Funding: This article is the result of the Science, Technology, and Innovation Project "Valorización de especies vegetales aromáticas comercializadas en la ciudad de Tarma para la obtención de compuestos volátiles usando tecnología de fluidos supercríticos" with code "P2-23-01-01", funded by "UNAAT INVESTIGA" led from the Vicepresidencia de Investigación of the Universidad Nacional Autónoma Altoandina de Tarma. M.A.A.Meireles thanks CNPq (309825-2020-2) for support with the English language.

Data Availability Statement: The data presented in this manuscript are part of the work submitted by Joselin Paucarchuco-Soto and German Pacahuala in partial fulfillment of the requirements for their degrees at the Universidad Autónoma Altoandina de Tarma (UNAAT, Peru). The data are available in the UNAAT repository: https://repositorio.unaat.edu.pe/handle/20.500.14514/121 (accessed on 12 May 2025).

Conflicts of Interest: The authors declare no conflict of interest.

References

1. Royal Botanic Gardens Kew *Schinus molle* L. | Plants of the World Online | Kew Science. Available online: https://powo.science.kew.org/taxon/urn:lsid:ipni.org:names:71044-1 (accessed on 11 February 2024).
2. Lalia, A.; Harizia, A.; Righi, K.; Daikh, Z.E. Chemical Composition and Allelopathic Potential of *Schinus molle* L. (Anacardiaceae) Essential Oils against Common Weeds of Wheat Crop. *Nat. Prod. Res.* **2025**, *39*, 682–688. [CrossRef] [PubMed]
3. Irahal, I.N.; Lahlou, F.A.; Hmimid, F.; Errami, A.; Guenaou, I.; Diawara, I.; Kettani-Halabi, M.; Fahde, S.; Ouafik, L.; Bourhim, N. Identification of the Chemical Composition of Six Essential Oils with Mass Spectroscopy and Evaluation of Their Antibacterial and Antioxidant Potential. *Flavour Fragr J.* **2021**, 465–476. [CrossRef]
4. Belhoussaine, O.; El Kourchi, C.; Harhar, H.; Bouyahya, A.; Yadini, A.E.; Fozia, F.; Alotaibi, A.; Ullah, R.; Tabyaoui, M. Chemical Composition, Antioxidant, Insecticidal Activity, and Comparative Analysis of Essential Oils of Leaves and Fruits of *Schinus molle* and *Schinus terebinthifolius*. *Evid.-Based Complement. Altern. Med.* **2022**, *2022*, 4288890.
5. Volpini-klein, A.F.N.; Júnior, S.E.L.; Cardoso, C.A.L.; Cabral, R.P.; Louro, G.M.; Coutinho, E.J.; de Jesus, D.A.; Junior, D.P.; Simionatto, E. Chemical Composition of Essential Oils from Leaves and Fruits of *Schinus molle* Obtained by Different Extraction Methods (Hydrodistillation, Fractional Hydrodistillation and Steam Distillation) and Seasonal Variations. *J. Essent. Oil Bear. Plants* **2021**, *24*, 228–242. [CrossRef]
6. Umay, A. Investigation of Chemical Composition and Phytotoxic Effects of Essential Oils Obtained from *Schinun Molle* Leaves and Resins. *Tome* **2022**, *75*, 26–33. [CrossRef]
7. Salas, J.M.Z.; Quiroz, K.D.A.; Miranda, L.F.C.; Sanchez, J.M.C. Use of Molle (*Schinus molle*) Essential Oil as a Biocide against Potato Aphid (*Macrosiphum euphorbiae*). *Neuro Quantology* **2022**, *20*, 5752–5759. [CrossRef]
8. Phiri, N.; Serame, E.L.; Pheko, T. Extraction, Chemical Composition, and Antioxidant Activity Analysis of Essential Oil from *Schinus molle* Medicinal Plant Found in Botswana. *Am. J. Essent. Oils Nat. Prod.* **2021**, *9*, 1–9.
9. Herrera-calderon, O.; Chavez, H.; Enciso-Roca, E.C.; Común-Ventura, P.W.; Hañari-Quispe, R.D.; Figueroa-Salvador, L.; Loyola-Gonzales, E.L.; Pari-Olarte, J.B.; Aljarba, N.H.; Alkahtani, S.; et al. GC-MS Profile, Antioxidant Activity, and In Silico Study of the Essential Oil from *Schinus molle* L. Leaves in the Presence of Mosquito Juvenile Hormone-Binding Protein (MJHBP) from *Aedes aegypti*. *Biomed. Res. Int.* **2022**, 5601531.
10. Quiroz, J.R.R.; Salvatierra, M.E.S. Composición Química y Actividad Antibacteriana de Los Aceitrs Esenciales de *Citrus Paradisi*, *Juglans Neotropica*, Diels, *Schinus molle* y *Tagetes Elliptica* Smith. *Rev. Soc. Química del Perú* **2021**, *87*, 228–241. [CrossRef]
11. Landero-valenzuela, N.; Alonso-hernández, N.; Lara-Viveros, F.; Gómez-Domínguez, N.S.; Juárez-Pelcastre, J.; Aguado-Rodríguez, J.; Luna-cruz, A.; Lagunez-Rivera, L.; Aguilar-Pérez, L.A.; Hinojosa-Garro, D.; et al. Efficiency of *Schinus molle* Essential Oil against *Bactericera cockerelli* (Hemiptera: Triozidae) and *Sitophilus zeamais* (Coleoptera: Dryophthoridae). *Agriculture* **2022**, *12*, 554. [CrossRef]
12. Mellak, N.; Ghali, N.; Messaoudi, N.; Benhelima, A.; Ferhat, M.; Addou, A. Study of Corrosion Inhibition Properties of *Schinus molle* Essential Oil on Carbon Steel in HCl. *Mater. Corros.* **2021**, *72*, 1270–1278. [CrossRef]
13. Morales-Rabanales, Q.N.; Coyotl-Pérez, W.A.; Rubio-Rosas, E.; Cortes-Ramírez, G.S.; Ramírez, J.F.S.; Villa-Ruano, N. Antifungal Properties of Hybrid Films Containing the Essential Oil of *Schinus molle*: Protective Effect against Postharvest Rot of Tomato. *Food Con* **2022**, *134*, 108766.
14. Sánchez, J.M.C.; Miranda, L.F.C.; Salas, J.M.Z.; Quiroz, K.D.A. Microencapsulation of Essential Oil of Molle (*Schinus molle*) against the Aphid Macrosiphum Euphorbiae. *J. Pharm. Negat. Results* **2022**, *13*, 1019–1023. [CrossRef]
15. Chavez-Marquez, E.; Bernedo, M.S.; Jara, E.M.; Quequezana-Bedregal, M.J.; Gutierrez-Oppe, E.E.; de Alcântara Pessôa Filho, P. Development of Intelligent and Active Potato Starch Films Based on Purple Corn Cob Extract and Molle Essential Oil. *Int. J. Biol. Macromol.* **2023**, *242*, 125080. [CrossRef]
16. Abdelgaleil, S.A.M.; El-sabrout, A.M. Composition, Toxicity and Developmental Potential of Three Essential Oils on the West Nile Virus Mosquito, *Culex pipiens* L. *Int. J. Pest Manag.* **2023**, *69*, 175–183. [CrossRef]
17. Gad, H.A.; Hamza, A.F.; Abdelgaleil, S.A.M. Chemical Composition and Fumigant Toxicity of Essential Oils from Ten Aromatic Plants Growing in Egypt against Different Stages of Confused Flour Beetle, *Tribolium confusum* Jacquelin Du Val. *Int. J. Trop. Insect Sci.* **2021**, *42*, 697–706. [CrossRef]

18. Hussein, H.S.; Tawfeek, M.E.; Abdelgaleil, S.A.M. Chemical Composition, Aphicidal and Antiacetylcholinesterase Activities of Essential Oils against *Aphis nerii* Boyer de Fonscolombe (Hemiptera: Aphididae). *J. Asia. Pac. Entomol.* **2021**, *24*, 259–265.
19. Belayneh, Y.M.; Mengistu, G.; Hailay, K. Evaluation of Hepatoprotective and Antidiarrheal Activities of the Hydromethanol Crude Extract and Solvent Fractions of *Schinus molle* L. (Anacardiaceae) Leaf and Fruit in Mice. *Metab. Open* **2024**, *21*, 100272. [CrossRef]
20. Mekuria, A.B.; Geta, M.; Birru, E.M.; Gelayee, D.A. Antimalarial Activity of Seed Extracts of *Schinus molle* Against *Plasmodium berghei* in Mice. *J. Evidence-Based Integr. Med.* **2021**, *26*. [CrossRef]
21. Aboalhaija, N.; Afifi, F.; Al-Hussaini, M.; Al-Najjar, M.; Abu-dahab, R.; Hasen, E.; Rashed, M.; Haq, S.A.; Khalil, E. *In Vitro* and *In Vivo* Evaluation of the Wound Healing Potential of the Extracts of *Schinus molle* L. (Anacardiaceae) Grown in Jordan. *Indian J. Pharm. Sci.* **2021**, *83*, 261–270.
22. Bvenura, C.; Kambizi, L. Composition of Phenolic Compounds in South African *Schinus molle* L. Berries. *Foods* **2023**, *11*, 1376.
23. Bekele, T.; Yimam, B.B. Phytochemical Screening and Antimicrobial Activity of Stem Bark Extracts of *Schinus molle Linens*. *Sch. Int. J. Chem. Mater. Sci.* **2023**, *6*, 108–114. [CrossRef]
24. Ovidi, E.; Garzoli, S.; Masci, V.L.; Turchetti, G.; Tiezzi, A. GC-MS Investigation and Antiproliferative Activities of Extracts from Male and Female Flowers of *Schinus molle* L. *Nat. Prod. Res.* **2021**, *35*, 1923–1927. [CrossRef]
25. Sánchez-Mendoza, M.E.; López-Lorenzo, Y.; Cruz-Antonio, L.; Arrieta-Baez, D.; Pérez-González, M.C.; Arrieta, J. First Evidence of Gastroprotection by *Schinus molle*: Roles of Nitric Oxide, Prostaglandins, and Sulfhydryls Groups in Its Mechanism of Action. *Molecules* **2022**, *27*, 7321. [CrossRef]
26. Hailan, W.A.; Al-Anazi, K.M.; Farah, M.A.; Ali, M.A.; Al-Kawmani, A.A.; Abou-Tarboush, F.M. Reactive Oxygen Species-Mediated Cytotoxicity in Liver Carcinoma Cells Induced by Silver Nanoparticles Biosynthesized Using *Schinus molle* Extract. *Nanomaterials* **2022**, *12*, 161. [CrossRef]
27. Valdiviezo-Campos, J.E.; Rodriguez-Aredo, C.D.; Ruiz-Reyes, S.G.; Venegas-casanova, E.A.; Bussmann, R.W.; Ganoza-yupanqui, M.L. Identification of Polyphenols by UPLC-MS/MS and Their Potential in Silico Antiviral Activity from Medicinal Plants in Trujillo, Peru. *J. Pharm. Pharmacogn. Res.* **2024**, *12*, 323–347.
28. Kim, M.J.; Kim, D.W.; Kim, J.G.; Shin, Y.; Jung, S.K.; Kim, Y. Analysis of the Chemical, Antioxidant, and Anti-Inflammatory Properties of Pink Pepper (*Schinus molle* L.). *Antioxidants* **2021**, *10*, 1062. [CrossRef]
29. Osman, E.E.A.; Morsi, E.A.; El-Sayed, M.M.; Gobouri, A.; Abdel-Hameed, E.-S.S. Identification of the Volatile and Nonvolatile Constituents of *Schinus molle* (L.) Fruit Extracts and Estimation of Their Activities as Anticancer Agents. *J. Appl. Pharm. Sci.* **2021**, *11*, 163–171. [CrossRef]
30. Erenler, R.; Chaoui, R.; Yildiz, I.; Genc, N.; Gecer, E.N.; Temiz, C.; Akkal, S. Biosynthesis, Characterisation, and Antioxidant Activity of Silver Nanoparticles Using *Schinus molle* L. *Trends Sci.* **2023**, *20*, 6105.
31. Mügge, F.L.B.; Morlock, G.E. Chemical and Cytotoxicity Profiles of 11 Pink Pepper (*Schinus* Spp.) Samples via Non-Targeted Hyphenated High-Performance Thin-Layer Chromatography. *Metabolomics* **2023**, *19*, 48. [CrossRef]
32. İlgün, S.; Karatoprak, G.Ş.; Polat, D.Ç.; Şafak, E.K.; Yücel, Ç.; İnce, U.; Uvat, H.Ö.; Akkol, E.K. Assessment of Phenolic Composition, Antioxidant Potential, Antimicrobial Properties, and Antidiabetic Activity in Extracts Obtained from *Schinus molle* L. Leaves and Fruits. *Front. Biosci. (Landmark Ed.)* **2023**, *28*, 353.
33. Feriani, A.; Tir, M.; Mufti, A.; Caravaca, A.M.G.; Contreras, M.D.M.; Taamalli, A.; Carretero, A.S.; Aldawood, N.; Nahdi, S.; Alwasel, S.; et al. HPLC-ESI-QTOF-MS/MS Profiling and Therapeutic Effects of *Schinus terebinthifolius* and *Schinus molle* Fruits: Investigation of Their Antioxidant, Antidiabetic, Anti-Inflammatory and Antinociceptive Properties. *Inflammopharmacology* **2021**, *29*, 467–481. [CrossRef]
34. Mengistu, G.; Hailay, K.; Misganaw, D.; Andualem, A.; Belayneh, Y.M. *In Vivo* Antidiarrheal Activities of the Hydro Alcoholic Extracts of *Schinus molle* L. (Anarcardiaceae) Leaf in Mice. *bioRxiv* **2022**. [CrossRef]
35. Pravalika, K.; Kulkarni, N.M.; Kumar, G.V.; Murali, S. Pharmacological Study of Analgesic Activity of *Schinus molle*. *J. Pharm. Negat. Results* **2022**, *13*, 8226–8231. [CrossRef]
36. Pintado, M.E.; Saraiva, J.M.A.; da Cruz Alexandre, E.M. *Technologies to Recover Polyphenols from AgroFood By-Products and Wastes*; Academic Press: Cambridge, MA, USA, 2022; ISBN 978-0-323-85273-9.
37. Santana, Á.L.; Paucar, L.O.C.; Veggi, P.C.; Viganó, J.; Meireles, M.A.A. Supercritical Fluid Extraction. In *Green Extraction Techniques in Food Analysis*; Bentham Science Publishers: Sharjah, United Arab Emirates, 2023; pp. 280–323.
38. Chañi-Paucar, L.O.; Santana, Á.L.; Albarelli, J.Q.; Meireles, M.A.A. Extraction of Polyphenols by Sub/Supercritical Based Technologies. In *Technologies to Recover Polyphenols from AgroFood By-Products and Wastes*; Academic Press: Cambridge, MA, USA, 2022; pp. 137–168. ISBN 9780323852739.
39. Barroso, M.S.T.; Villanueva, G.; Lucas, A.M.; Perez, G.P.; Vargas, R.M.F.; Brun, G.W.; Cassel, E. Supercritical Fluid Extraction of Volatile and Non-Volatile Compounds from *Schinus molle* L. *Brazilian J. Chem. Eng.* **2011**, *28*, 305–312. [CrossRef]
40. Marongiu, B.; Porcedda, A.P.S.; Casu, R.; Pierucci, P. Chemical Composition of the Oil and Supercritical CO_2 Extract of *Schinus molle* L. *Flavour Fragr. J.* **2004**, *19*, 554–558. [CrossRef]

41. Prado, J.M.; Prado, G.H.C.; Meireles, M.A.A. Scale-up Study of Supercritical Fluid Extraction Process for Clove and Sugarcane Residue. *J. Supercrit. Fluids* **2011**, *56*, 231–237.
42. ANSI-ASAE Method of Determining and Expressing Particle Size of Chopped Forage Materials by Screening. In *ASAE STANDARDS*; EUA: Brussels, Belgium, 1998; pp. 562–564.
43. NIST-National Institute of Standards and Technology Propiedades Termofísicas de Sistemas Fluidos. Available online: https://webbook.nist.gov/chemistry/fluid/ (accessed on 28 October 2024).
44. Martínez, J.; Monteiro, A.R.; Rosa, P.T.V.; Marques, M.O.M.; Meireles, M.A.A. Multicomponent Model to Describe Extraction of Ginger Oleoresin with Supercritical Carbon Dioxide. *Ind. Eng. Chem. Res.* **2003**, *42*, 1057–1063. [CrossRef]
45. Santana, Á.L.; Albarelli, J.Q.; Santos, D.T.; Souza, R.; Machado, N.T.; Araújo, M.E.; Meireles, M.A.A. Kinetic Behavior, Mathematical Modeling, and Economic Evaluation of Extracts Obtained by Supercritical Fluid Extraction from Defatted Assaí Waste. *Food Bioprod. Process.* **2018**, *107*, 25–35. [CrossRef]
46. Meireles, M.A.A. Extraction of Bioactive Compounds from Latin American Plants. In *Supercritical Fluid Extraction of Nutraceuticals and Bioactive Compounds*; Martinez, J., Ed.; CRC Press—Taylor & Francis Group: Boca Raton, FL, USA, 2008; pp. 243–274.
47. Esquível, M.M.; Bernardo-Gil, M.G.; King, M.B. Mathematical Models for Supercritical Extraction of Olive Husk Oil. *J. Supercrit. Fluids* **1999**, *16*, 43–58. [CrossRef]
48. Bendif, H.; Miara, M.D.; Kalboussi, Z.; Grauzdytė, D.; Povilaitis, D.; Venskutonis, P.R.; Maggi, F. Supercritical CO_2 Extraction of *Rosmarinus eriocalyx* Growing in Algeria: Chemical Composition and Antioxidant Activity of Extracts and Their Solid Plant Materials. *Ind. Crops Prod.* **2018**, *111*, 768–774. [CrossRef]
49. Scopel, R.; Neto, R.G.; Falcão, M.A.; Cassel, E.; Vargas, R.M.F. Supercritical CO_2 Extraction of *Schinus molle* L. with Co-Solvents: Mathematical Modeling and Antimicrobial Applications. *Braz. Arch. Biol. Technol.* **2013**, *56*, 513–519. [CrossRef]
50. Essien, S.O.; Young, B.; Baroutian, S. Recent Advances in Subcritical Water and Supercritical Carbon Dioxide Extraction of Bioactive Compounds from Plant Materials. *Trends Food Sci. Technol.* **2020**, *97*, 156–169. [CrossRef]
51. de Melo, S.A.V.; Costa, G.M.; Viana, A.C.; Pessoa, F.L. Computation of Crossover Pressure for Synthesis of Supercritical Fluid Separation Systems. In *10th International Symposium on Process Systems Engineering: Part A*; de Brito Alves, R.M., do Nascimento, C.A.O., Biscaia, E.C., Eds.; Computer Aided Chemical Engineering; Elsevier: Amsterdam, The Netherlands, 2009; Volume 27, pp. 399–404.
52. Lemmon, E.W.; Bell, I.H.; Huber, M.L.; McLinden, M.O. *Thermophysical Properties of Fluid Systems*; Linstrom, P.J., Mallard, W.G., Eds.; National Institute of Standards and Technology: Gaithersburg, MD, USA, 2024.
53. Chañi-Paucar, L.O.; Flores Johner, J.C.; Zabot, G.L.; Meireles, M.A.A. Technical and Economic Evaluation of Supercritical CO_2 Extraction of Oil from Sucupira Branca Seeds. *J. Supercrit. Fluids* **2022**, *181*, 105494. [CrossRef]
54. Santos, P.H.; Baggio Ribeiro, D.H.; Micke, G.A.; Vitali, L.; Hense, H. Extraction of Bioactive Compounds from Feijoa (*Acca Sellowiana* (O. Berg) Burret) Peel by Low and High-Pressure Techniques. *J. Supercrit. Fluids* **2019**, *145*, 219–227. [CrossRef]
55. Mukherjee, P.K. Bioactive Phytocomponents and Their Analysis. *Qual. Control Eval. Herb. Drugs* **2019**, 237–328. [CrossRef]
56. Paucarchuco Soto, J.; Padilla Pacahuala, G. *Evaluación de La Capacidad Antioxidante y Composición de Metabolitos Bioactivos Del Extracto Aromático Obtenido de Las Hojas de Schinus molle L. Con CO_2 Supercrítico*; Universidad Nacional Autónoma Altoandina de Tarma (UNAAT): Tarma, Peru, 2024.
57. Pereira, C.G.; Meireles, M.A.A. Supercritical Fluid Extraction of Bioactive Compounds: Fundamentals, Applications and Economic Perspectives. *Food Bioprocess Technol.* **2010**, *3*, 340–372. [CrossRef]
58. Bhattacharyya, S.; Sarma, S.D.; Dutta, P.; Begum, T.; Lal, M.; Perveen, K.; Bukhari, N.A. Insights into *Citrus limon* (L.) Osbeck Peel Essential Oil from NE India: A Study of Its Pharmacological Properties and Chemical Composition. *J. Essent. Oil Bear. Plants* **2024**, *27*, 1362–1376. [CrossRef]
59. St-Gelais, A.; Mathieu, M.; Levasseur, V.; Ovando, J.F.; Escamilla, R.; Marceau, H. Preisocalamendiol, Shyobunol and Related Oxygenated Sesquiterpenes from Bolivian *Schinus molle* Essential Oil. *Nat. Prod. Commun.* **2016**, *11*, 547–550. [CrossRef]
60. Govindarajan, M.; Benelli, G. Eco-Friendly Larvicides from Indian Plants: Effectiveness of Lavandulyl Acetate and Bicyclogermacrene on Malaria, Dengue and Japanese Encephalitis Mosquito Vectors. *Ecotoxicol. Environ. Saf.* **2016**, *133*, 395–402. [CrossRef]
61. Carroll, J.F.; Paluch, G.; Coats, J.; Kramer, M. Elemol and Amyris Oil Repel the Ticks *Ixodes scapularis* and *Amblyomma americanum* (Acari: Ixodidae) in Laboratory Bioassays. *Exp. Appl. Acarol.* **2010**, *51*, 383–392. [CrossRef]
62. Moriasi, G.; Ngugi, M.; Mwitari, P.; Omwenga, G. Antioxidant, Anti-Prostate Cancer Potential, and Phytochemical Composition of the Ethyl Acetate Stem Bark Extract of *Boascia coriacea* (Pax.). *PLoS ONE* **2024**, *19*, e0309258. [CrossRef]
63. Seixas, P.T.L.; Demuner, A.J.; Barbosa, L.C.A.; Cerceau, C.I.; Blank, D.E.; Santos, M.H.D.; de Sá Farias, E.; Picanço, M.C. Chemical Composition and Larvicidal Activity of Essential Oils of Three Artemisia Species. *J. Appl. Entomol.* **2023**, *147*, 116–125. [CrossRef]
64. Sirichaiwetchakoon, K.; Lowe, G.M.; Kupittayanant, S.; Churproong, S.; Eumkeb, G. *Pluchea indica* (L.) Less. Tea Ameliorates Hyperglycemia, Dyslipidemia, and Obesity in High Fat Diet-Fed Mice. *Evid.-Based Complement. Altern. Med.* **2020**, *2020*, 8746137. [CrossRef]

65. de Lima Nunes, T.A.; Costa, L.H.; De Sousa, J.M.S.; De Souza, V.M.R.; Rodrigues, R.R.L.; Val, M.D.C.A.; Pereira, A.C.T.d.C.; Ferreira, G.P.; Da Silva, M.V.; Da Costa, J.M.A.R.; et al. *Eugenia piauhiensis* Vellaff. Essential Oil and γ-Elemene Its Major Constituent Exhibit Antileishmanial Activity, Promoting Cell Membrane Damage and *in vitro* Immunomodulation. *Chem. Biol. Interact.* **2021**, *339*, 109429. [CrossRef]
66. Chen, W.; Lu, Y.; Wu, J.; Gao, M.; Wang, A.; Xu, B. Beta-Elemene Inhibits Melanoma Growth and Metastasis via Suppressing Vascular Endothelial Growth Factor-Mediated Angiogenesis. *Cancer Chemother. Pharmacol.* **2011**, *67*, 799–808. [CrossRef]
67. Gao, L.; Wei, Y.; Li, K.; Chen, J.; Wang, P.; Du, J.; Peng, J.; Gao, Y.; Zhang, Z.; Liu, Y.; et al. *Perilla Frutescens* Repels and Controls *Bemisia Tabaci* MED with Its Key Volatile Linalool and Caryophyllene. *Crop Prot.* **2024**, *184*, 106837. [CrossRef]
68. Bhatia, S.P.; Letizia, C.S.; Api, A.M. Fragrance Material Review on Elemol. *Food Chem. Toxicol.* **2008**, *46*, S147–S148. [CrossRef]

Disclaimer/Publisher's Note: The statements, opinions and data contained in all publications are solely those of the individual author(s) and contributor(s) and not of MDPI and/or the editor(s). MDPI and/or the editor(s) disclaim responsibility for any injury to people or property resulting from any ideas, methods, instructions or products referred to in the content.